NAVORD REPORT 2954

DRAG AND EVAPORATION OF DRY ICE MODELS IN

SUPERSONIC AIR FLOW

21 SEPTEMBER 1953

U. S. NAVAL ORDNANCE LABORATORY

WHITE OAK, MARYLAND

Aeroballistic Research Report 189

DRAG AND EVAPORATION OF DRY ICE MODELS IN SUPERSONIC AIR FLOW

By:

K. B. Gruenewald

ABSTRACT: Investigations on drag and evaporation
of dry ice models were conducted in the NOL 40 x
40 cm Aeroballistics Tunnel No. 2. The drag coef-
ficient was determined for dry ice spheres at Mach
numbers 2.9 and 4.3, and the rate of evaporation of
dry ice was investigated on cubes and spheres at
Mach numbers 1.9, 2.9 and 4.3. The drag coefficient
was found to be essentially the same as that of usual
nonevaporative wind-tunnel models of the same geometric
shape. Most of the evaporation during a blow occurred
at the front portion of the model. In this wind tunnel
the mass loss caused by evaporation becomes smaller
as the Mach number is increased due to the lower
density of the air in the test section at higher Mach
numbers. Furthermore, the mass loss per unit cross-
sectional area of the model decreases with increasing
model size.

U. S. NAVAL ORDNANCE LABORATORY
WHITE OAK, MARYLAND

NAVORD Report 2954   21 September 1953

This report presents results of experiments on evaporating models. The investigation was suggested by
Prof. F. L. Whipple, Harvard University, Cambridge,
Massachusetts, in connection with his studies on
meteors. The results of this investigation have been
evaluated with respect to their application to astrophysical phenomena by R. N. Thomas and F. L. Whipple
and are partially published in references (a) and (b).
Since experimental results on evaporating models may
also be of interest to problems of missile cooling,
the investigation on dry ice models is presented in
all details in this report.

This investigation was made under NOL task number
Re9a-108. The measurements were carried out at the
Naval Ordnance Laboratory in the 40 x 40 cm Aeroballistics Tunnel No. 2 in 1950.

The author wishes to express his gratitude to
Mr. J. M. Kendall and Mr. J. L. Ettle who worked out
the technique of manufacturing the dry ice models and
who prepared all the models used during this investigation. The author acknowledges the help of
Mr. M. Peucker in preparing the drag balance.

EDWARD L. WOODYARD
Captain, USN
Commander

R. H. KURZWEG, Chief
Aeroballistic Research Department
By direction

CONTENTS

TABLES AND ILLUSTRATIONS

DRAG AND EVAPORATION OF DRY ICE MODELS IN SUPERSONIC AIR FLOW

I. INTRODUCTION

1. A theory for determining air densities at high altitudes from meteoric data has been developed by F. L. Whipple (reference c). The application of this theory requires the knowledge of the numerical values of two quantities, namely aerodynamic drag and mass loss of meteors which have to be estimated. In order to substantiate the quantitative aspect of this theory, Professor Whipple (reference d) suggested the experimental investigation of evaporation rate and drag of vaporizing models in a supersonic wind tunnel. An accuracy of the test results within 50 per cent of the actual values was considered sufficient to satisfy the theory.

2. The temperature of the atmosphere at 50 km altitude amounts to about 350°K. For a meteor travelling at a speed of 50 km/sec at this altitude (reference e), the stagnation temperature of the air is approximately 10^6°K (reference f). The temperature of the meteor was assumed to be 2000°K, and the meteor was considered to vaporize from the solid state (sublimation) (reference d). In order to simulate these conditions at low temperatures, dry ice (solid CO_2) was chosen as the model material for the wind-tunnel measurements. Dry ice has a sublimation point of 194.7°K at 1 atm (reference g), which is intermediate between the wind-tunnel stagnation temperature of about 300°K and the static temperature of the air flow (177°K for Mach number 1.36 to about 50°K for Mach number 5.0).

II. TEST ARRANGEMENT

3. The investigation was performed in the NOL 40 x 40 cm Aeroballistics Tunnel No. 2 (reference h). For this tunnel the air is taken from the atmosphere, passed through a dryer which dries to a dewpoint of approximately -30°C, expanded in a Laval nozzle, and discharged through a supersonic diffuser into a vacuum vessel of 2000 m^3 volume. The tunnel is of the

intermittent type with 40 to 60 seconds blowing time
and has a nozzle exit cross section of 40 x 40 cm.
The Mach numbers and models investigated are shown
in Table I.

TABLE I

INVESTIGATED DRY ICE MODELS

Mach Number	Sphere Diameter in mm			Cube Side Length in mm		
1.86	$30^{\triangle}$	50^X	--	30^X	50^X	--
2.87	$30^{\triangle}$	50	70^X	30^X	50^X	70^X
4.25	--	50	--	--	--	--
x) Evaporation rate measurements only						

4.   High Mach numbers with low air densities would
best simulate the conditions encountered by meteors
in the upper atmosphere. However, at Mach number
4.25, the highest Mach number used, the duration of
a tunnel blow was already too short to produce a
mass loss sufficiently great to cause a visible
change in the model shape. Drag measurements have
been obtained in two cases only, since in the course
of the investigation the balance for the drag meas-
urements become inoperative. The mass loss was
determined in all cases.

5.   The dry ice model was mounted on a precooled
holder of small heat conductivity (bakelite) in
order to reduce evaporation of dry ice by heat con-
duction through the holder. The holder covered the
front portion of an axial force balance having 5 kg
load capacity (Figure 1). The spring deflection
during the blow caused by the air forces effects the
resistance of the strain gages attached to the
springs. The current due to the change of the
resistance was measured by a GE potentiometer recorder.
The balance was calibrated with model-holder and a
ring of dry ice around the holder screw provided to
hold the model. In this manner errors caused by the
low temperature of the dry ice model were eliminated
as far as possible.

6.   The mass loss due to the vaporization during
the blow was determined by weighing the models
before and after the blow. This loss was corrected
by the mass loss experienced during an equal handling
period without blast.

III. TEST PROCEDURE

A.   Manufacturing of the models

7.   The dry ice was sawed into cubes and in each
cube a hole with threads was cut using a tap pre-
cooled in a mixture of dry ice and alcohol. Then
the cube was screwed on a precooled sting of bake-
lite mounted on a lathe and was cut to a sphere with
a knife.

B.   Test

8.   The model was weighed quickly lying on filter
paper in order to reduce mass loss due to heat con-
duction to the scales. At the moment the weight was
determined a stop clock was turned on. After the
diameter of the model had been measured with a
caliper, the model was screwed on the precooled bake-
lite sting covering the front portion of the balance.
(This sting was precooled by an attached dry ice
piece.) Then the balance was adjusted and the blow
started. Another stop clock measured the blow time.
The drag was recorded during the blow with the GE
recorder. After the blow the model was taken out of
the tunnel and weighed again. The stop clock was
turned off when this second weighing was finished.
Finally the diameter of the model was measured again.
The time between the end of the blow and the end of
the second weighing was determined with a watch.
Supply air pressure and temperature were measured for
the determination of the drag coefficient.

C.   Mass loss without blow

9.   The procedure for determining the mass loss
without blow was the same as just described but
without blow and drag measurements. This mass loss
was determined for cubes and spheres with different
side lengths or diameters and also for different
evaporation times.

IV. DATA REDUCTION

10. The drag coefficient of the model was deter-
mined at the start and the end of the blow only
and the evaporated mass was determined for the
time duration of one blow. The following steps
were taken for this procedure:

A. Diameter at start and end of the test

11. The model diameter at the start and the end
of the test (first and last weighing of the model)
was measured by a caliper. These measurements
are inaccurate in so far as the caliper melts dry
ice during the time it touches the model and there-
fore indicates a diameter smaller than the actual
diameter. The inaccuracy is larger for spheres
than for cubes because the caliper touches the
sphere in two points, which melt quickly, but
touches the cube along two sides which melt more
slowly. This was confirmed by comparison of the
measured diameters of the spheres with the diameters
calculated from the weight of the models at the test
start under the assumption that the models were true
spheres and cubes, and taking into account the weight
of the sting hole in the models (The specific weight
of the dry ice used was determined to be 1.52 g/cm^3.)
The calculated side lengths of the cubes agreed with
the measured ones within less than 1 per cent; the
calculated values of the sphere diameters were about
1 per cent to 2 per cent larger than the measured
values. Considering the inaccuracy of the measurements,
the calculated values of the diameters were taken at
the test start. Since the shape of the models changed
unsymmetrically during the blow, only the measured values
of the diameter at the end of the test could be used for
the data evaluation. However, 0.3 mm corresponding to
about 1 per cent of the diameter of the smallest sphere
have been added as a correction to the measured values
of the sphere diameter according to the above mentioned
experience.

B. Diameter at start and end of the blow

12. These diameters were obtained from the diameters
at start and end of the test, deducting and adding the
experimentally determined diameter decrease for the
time while not blowing respectively.

13. This time consists of two parts; the time
between the first weighing of the model and the
blow start and the time between blow end and second
weighing. These time intervals were determined from
the blow time, the time between first and second
weighing and the time between blow end and second
weighing all of which were known.

14. Furthermore, the mass loss of spheres and
cubes for times without blow was known. The diameter
decrease of the models without blow was determined
and is shown in Figure 2. It was obtained from the
measured and calculated diameters of the model at
the start and the end of the test without blow.
Figure 2 shows that the scatter of the calculated
values is less than that of the measured values, as
explained above. The diameter decrease as a function
of the diameter at test start for a constant time
interval is shown in Figure 2a. One curve for all
models was used since the diameter decrease was found
to be independent of the model size within the measuring
accuracy. The average scatter of the calculated values
is about ±7 per cent.

C. Drag coefficient

15. Since the diameters of the model at the start
and the end of the blow are determined, the correspond-
ing cross-section areas A are known. The density ρ
and the velocity v of the undisturbed flow were deter-
mined from the pressure and temperature of the supply
air and the Mach number. The drag coefficient C_D was
calculated using the equation:

$$C_D = \frac{F}{\frac{\rho \cdot v^2}{2} A}$$

where F is the drag force.

D. Mass loss while not blowing

16. The mass loss per unit time and unit surface area
without blow was found to be the same for cubes and
spheres; namely, 0.000283 g/sec. cm^2 ± 6 per cent.
However, the mass loss without blow referred to the
cross-sectional area is different for cubes and spheres
(see Table 3). To facilitate data reduction, the mass
loss was referred to the cross-sectional area of the

models since the area perpendicular to the air
stream did not change much as compared with that
of the model surface during the blow (Figure 3 and
Table II). Furthermore, it was difficult to deter-
mine the model surface area after the blow.

17. The mass loss for the time between test start
and blow start was obtained by multiplying the mass
loss without blow (in g/sec. cm² area) with the time
without blow and with the average cross-sectional
area which the model had during this time. The same
was done for the time between blow end and test end.
Both mass losses added together give the total mass
loss while not blowing. The procedure of determining
the mass loss after the blow is somewhat inaccurate
because the model shape after the blow is not a sphere
or a cube respectively. This procedure was chosen,
however, because the average surface area of the model
after the blow was very difficult to determine and
because the time between blow end and test end was
in no case more than 31 per cent of the total time
without blow.

4. Mass loss during blow

18. This loss was obtained by deducting the loss
while not blowing from the total loss between the
two weighings. The mass loss was referred to one
second blow time and to one cm² of the average cross-
sectional area of the model perpendicular to the air
stream during blow time.

V. ACCURACY OF THE MEASUREMENTS

19. The calibration of the balance showed that it
was influenced by sideforces such as lift and yaw. The
measurement obtained from a sideforce was about 20 per
cent of the value resulting from a force of the same
magnitude acting axially. In spite of this inaccuracy,
this balance was used because no other balance was
available at that time. Furthermore, since the model
shapes at least at the start of the blow were symmetrical
with respect to the air stream, any sideforce influence
could be considered negligible. The holder influence on
the drag measurements could not be eliminated completely
but this influence is considered to be small and may be
neglected for these models. The approximate accuracies
for the mass losses during the blow were calculated with
the following assumed errors in determining the test items:

Weight ± 0.1 g

Time between weighings ± 1 sec.

Time without blast between test start
and blow start ± 5 sec.

Time without blast between blow end
and test end ± 5 sec.

Blow time ± 0.2 sec.

Diameter decrease without blast (as
found experimentally) ± 7 per cent

Mass loss without blast per second
and cm^2 cross-sectional area (as
found experimentally) ± 6 per cent

Diameter at test start and end
± 0.3 mm for spheres

Edge length at test start and end
± 0.1 mm for cubes

The error in the determination of the average
cross-sectional area of the models during the blow
was calculated to be less than 1 per cent for a cube
of 70 mm side length and up to 2.5 per cent for a
sphere 30 mm diameter. The mass loss per second and
cm^2 of this area was found to be accurate to ± 5 per
cent at Mach number 1.86 and up to ± 17 per cent at
Mach number 4.25. The measured values of the mass
loss for all models and all Mach numbers scatter
within ± 11 per cent around the curves drawn in
Figure 4. At Mach number 1.86 there exists a distinct
difference between cubes (scatter ± 5 per cent) and
spheres (scatter ± 16 per cent). The high value of
scattering of the spheres may be attributed to loss
of pieces broken off from the spheres during the blow.
(See values with question marks in Figure 4).

VI. RESULTS

20. The vaporization of dry ice at Mach number 4.25
was so small that no change in model shape could be
observed. At the lower Mach numbers 2.87 and 1.86
the evaporation was clearly visible. During evaporation,

the front part of the models assumed a conical shape
with a round tip and nicks in case of the spheres and
formed sloping areas with nicks in case of the cubes.
The rear part of each model remained unchanged. The
somewhat non-uniform evaporation at the front part may
be caused by inhemogeneities of the polycrystalline
structure of the dry ice, due to the mechanical com-
pacting of the snow flakes in making solid dry ice.
The shapes of models with 5 cm diameter after the
blow are shown in Figure 3 (one cylindrical model,
5 cm long and 3 cm in diameter, was also investigated
and is shown in Figure 3). Models 3 cm in diameter
showed more erosion of shapes (half spherical shape
in the case of spheres), models with 7 cm diameter were
less eroded as the models shown in Figure 3.

21.   The drag coefficient of dry ice spheres was
found to be approximately 1 at Mach numbers 4.25 and
2.87, measured 3 to 4 sec. after the blow started.
The coefficient increased 5 per cent at Mach number
4.25 and 16 per cent at Mach number 2.87 during the
blow with a duration of about 35 seconds (Table 3).
The drag coefficient shortly after blow start is in
fair agreement with the drag coefficient of spheres
measured in supersonic wind tunnels. The increase
of the drag coefficient during the blow can be
attributed to the variation of the shape of the
model and seems to be unaffected by the evaporation
of dry ice surrounding the model. Thus the drag
coefficient seems to be the same as found for non-
evaporative wind-tunnel models of the same shape.
Because the shape changes during the blow from
spheres to hemispheres (especially at low Mach
numbers), the drag coefficient can be expected to
be between 1 and 1.5.

22.   The mass loss during the evaporation as a
function of the average cross-sectional area of the
model during the blow is shown in Figure 4. The values
for the spheres and those of the cubes have been found
to be approximately equal at each Mach number. Some
previous unpublished data by J. M. Kendall and
P. P. Wegener of NOL taken at a Mach number of 1.7 in
a continuous 2.5 x 2.5 cm wind tunnel are included in
Figure 4. The graph shows that the mass loss due to
the evaporation of dry ice increases with decreasing
Mach number and with decreasing area.

23.   The evaporation of dry ice in supersonic air
flow may be explained as follows: The evaporation

of dry ice is due to the transfer of heat from the
air to the model and to the transfer of evaporated
material from the model to the air. The high rate
of energy exchange with the oncoming air at the
front part of the model causes a great evaporation
of dry ice. The evaporating process is supported
by the quick replacement of evaporating dry ice
molecules by air molecules. The number of air
molecules per unit time is a function of air density
and velocity. At the rear of the model the energy
exchange is smaller. The mass transfer occurs mainly
by diffusion of dry ice molecules to the air stream.
Therefore this part of the model shows a much smaller
change in shape during the blow than the front part.
At lower Mach numbers more dry ice evaporates due
to the higher air densities.

24. There exist two possible explanations for the
dependency of the evaporation rate on the model size.
(a) The average thickness of the CO_2 air layer on
the small model is smaller than on the large model,
thus allowing a larger energy exchange relative to
the size of the model. (b) Heat conducted from the
model holder through the sting to the model has a
greater influence on the overall evaporation from
smaller models than from larger ones.

VII. CONCLUSIONS

25. The drag coefficient of dry ice spheres was
found to be 1 at Mach numbers 4.25 and 2.87. It
increased during the blow by 5 per cent at Mach number
4.25 and by 16 per cent at Mach number 2.87 due to the
change of the sphere shape caused by evaporation.
Within the accuracy of the drag measurements, the drag
coefficient of dry ice models can be considered to be
equal the drag coefficient of usual non-evaporative
wind-tunnel models of the same shape. No influence of
the evaporated CO_2 cloud on this coefficient was found.

26. The highest evaporation rate of CO_2 occurs on the
front part of the models, showing a considerable change
in the model shape in this region.

27. The specific mass loss due to the evaporation
decreases with increasing model sizes and is the same
for cubes and spheres within the measurement accuracy.
Furthermore the specific mass loss increases with
decreasing Mach numbers due to the increasing air
densities in the test section of the tunnel.

VIII.   REFERENCES

a.   Thomas, R. N. and Whipple, F. L., "The
Physical Theory of Meteors. II. Astroballistic
Heat Transfer", The Astrophysical Journal, 114,
448, (1951)

b.   Thomas, R. N. and Whipple, F. L., "Astroballistic
Heat Transfer", Journal of Aeronautical Sciences,
18, 636 (1951)

c.   Whipple, F. L., "Meteors and the Earth's Upper
Atmosphere", Reviews of Modern Physics, 15,
246 (1943)

d.   Communications with Professor Whipple

e.   Kuiper, G. P., "The Atmospheres of the Earth
and Planets", p. 149, Chicago 1949

f.   Warfield, C. N., "Tentative Tables for the
Properties of the Upper Atmosphere",
NACA TN 1200 pp. 45, 51, Washington 1947

g.   Lange, N. A., "Handbook of Chemistry", p. 1205,
Sandusky, Ohio (1941)

h.   Lightfoot, J. R., "The Naval Ordnance Laboratory
Aeroballistic Research Facility", Naval Ordnance
Laboratory Report (NOLR) No. 1079 (1950)

TABLE II

AVERAGE DECREASE OF THE MODEL DIAMETER[1] PERPENDICULAR TO THE AIR

STREAM DURING TEST[2] AND DURING BLOW

Model	Mach Number	Diameter at Test Start	Diameter Loss During Test	Test Time[2]	Diameter at Blow Start	Diameter Loss During Blow	Blow Time
		mm	%	sec.	mm	%	sec.
sphere	4.25	48.3	4.4	475	46.9	1.1	35.3
	2.87	30.3	6.8	270	29.7	3.9	35.0
		50.6	5.1	325	49.7	2.9	37.7
		70.7	3.2	278	70.0	1.9	35.0
	1.86	31.2	12.8	297	30.5	9.8	35.0
		50.2	7.4	332	49.6	5.2	35.1
cube[3]	2.87	31.3	6.4	224	30.9	4.1	35.1
		49.8	4.5	399	48.6	1.8	35.2
		70.5	2.6	382	69.4	0.8	35.4
	1.86	31.0	10.5	280	30.3	5.3	35.1
		49.9	5.3	286	49.2	3.5	35.1
cylinder	2.87	31.0	4.0	230	30.5	1.6	35.1

1) All given values are average values
2) Time between first and second weighing of the model
3) Diameter means side length of cube

TABLE III   DRAG COEFFICIENT AND MASS LOSS OF DRY ICE MODELS

Mo Undisturbed flow	Wind Tunnel Data	Model shape	Approx. model diameter[1] cm	Ave. deviat. of dia.[2] %	Drag Coeff. C_D (blow's incl.)	Ave. deviat. of C_D %	Drag Coeff. C_D (blow excl.)	Ave. deviat. of C_D %	Number of tests	Mass loss during blow[3] g/s·cm²	Ave. deviat.[4] %	No. of tests
0	barom. press. (mm Hg) 760 / temperature (°K) 297 / Mass loss referred to surface area of spheres and cubes: (g/sec. cm²) 0.000283 ± 6%	sphere / cube	4 to 7 / 3 to 5	-- / --						0.00113[5] / 0.00170[5]		10 / 5
1.86	supply pressure (mm Hg) 748 / temp. (°K) 284 / in undisturbed flow: / velocity (m/sec.) 483 / pressure (mm Hg) 119 / temperature (°K) 168 / density (kg·s²·m⁻⁴) 0.0335	sphere / " / cube / "	2.9 / 4.8 / 2.9 / 4.8	3 / 2 / 3 / 1	-- / -- / -- / --	--	--	--	--	0.0494 / 0.0496 / 0.0515 / 0.0433	21 / 14 / 6 / 4	4 / 4 / 3 / 3
2.87	supply pressure (mm Hg) 764 / temp. (°K) 283 / in undisturbed flow: / velocity (m/sec.) 594 / pressure (mm Hg) 25.3 / temperature (°K) 106 / density (kg·s²·m⁻⁴) 0.0112	sphere / " / " / cube / " / " / cyl. (5cm lg)	2.9 / 4.8 / 6.9 / 3.0 / 4.8 / 6.9 / 3.0	2 / 6 / 1 / 1 / 2 / 1 / --	-- / 0.97 / -- / -- / -- / -- / --	8	1.12	9	2	0.0257 / 0.0199 / 0.0147 / 0.0256 / 0.0190 / 0.0181 / 0.0393	11 / 12 / 8 / 15 / 16 / 9 / --	3 / 5 / 3 / 3 / 4 / 3 / 1
4.25	supply pressure (mm Hg) 753 / temp. (°K) 288 / in undisturbed flow: / velocity (m/sec.) 673 / pressure (mm Hg) 3.6 / temperature (°K) 62 / density (kg·s²·m⁻⁴) 0.00272	sphere	4.7	6	1.00	2	1.14	3	9	0.00950	17	10

1) Ave. diameter during blow. Diameter in case of cube is substituted by average length of edge
2) Ave. deviation of diameter of the single tests vs. ave. diameter as given in column 4.
3) Mass loss is referred to 1 second blowing time and 1 cm² cross-sectional area of the model.
4) Deviation of mass loss of the single tests vs. Ave. loss as given in column 11.
5) Mass loss without blow.

FLOW DIRECTION

MODEL

MODEL HOLDER
(BAKELITE)

BALANCE SPRINGS

BALANCE HOLDER

BALANCE
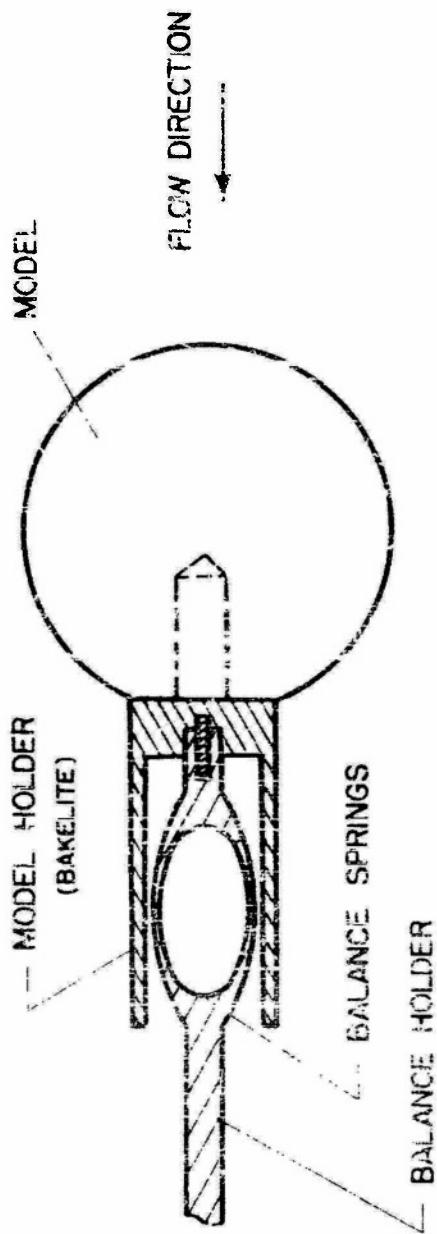
FIG. I   MODEL MOUNTING

13

Fig. 2a
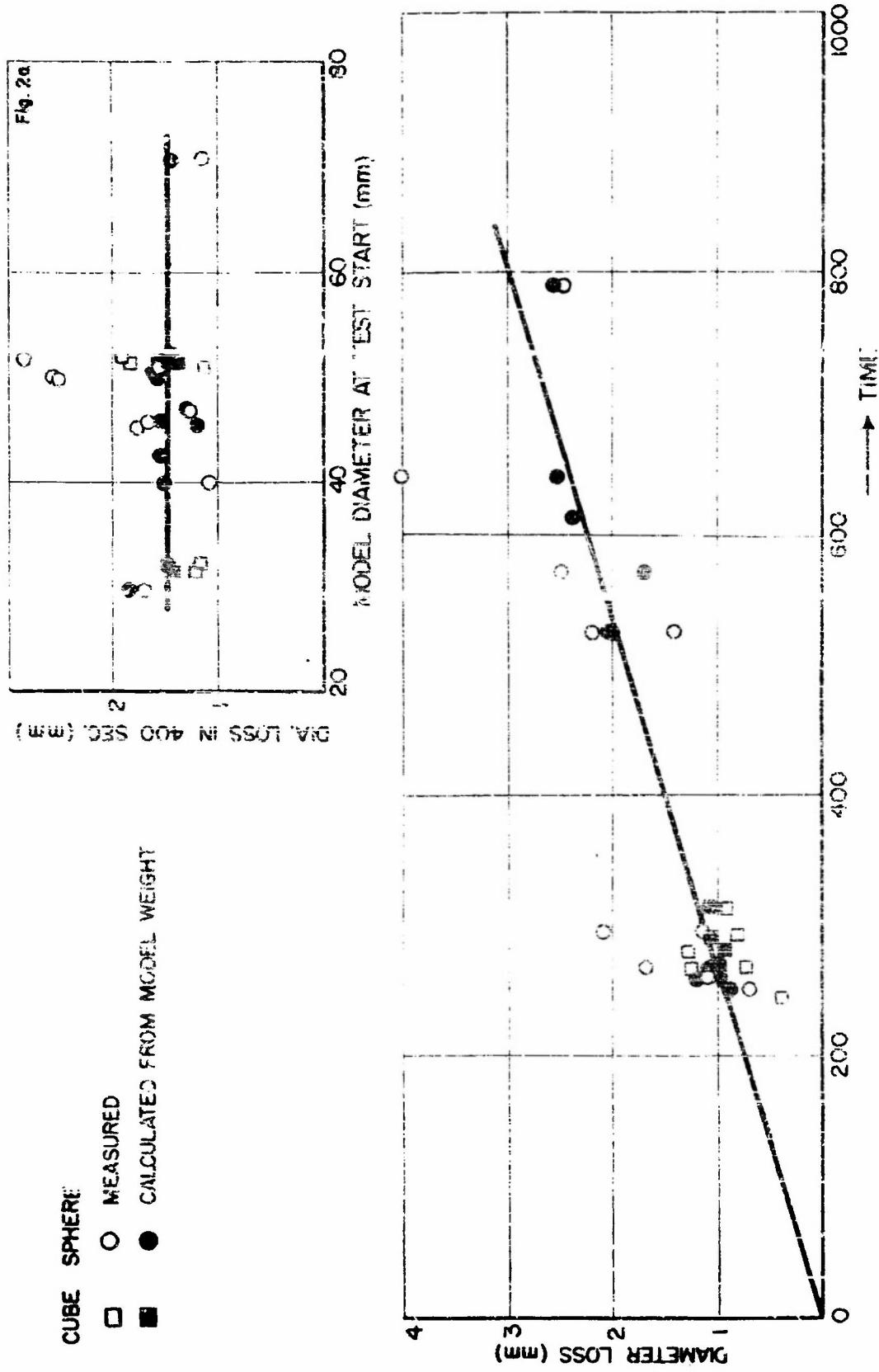
FIG. 2 DIAMETER DECREASE OF DRY ICE SPHERES AND CUBES WITHOUT BLOW

14

FLOW DIRECTION

←
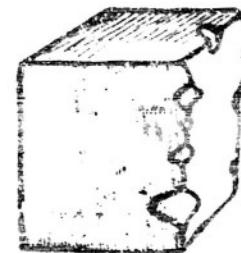

MACH NUMBER 2.87
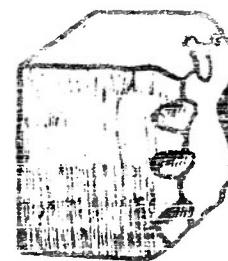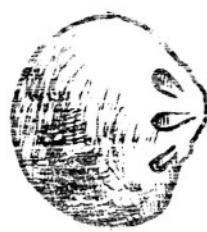
SPHERE   CUBE

CYLINDER

MACH NUMBER 1.86

FIG. 3 MODEL SHAPES AT BLOW END
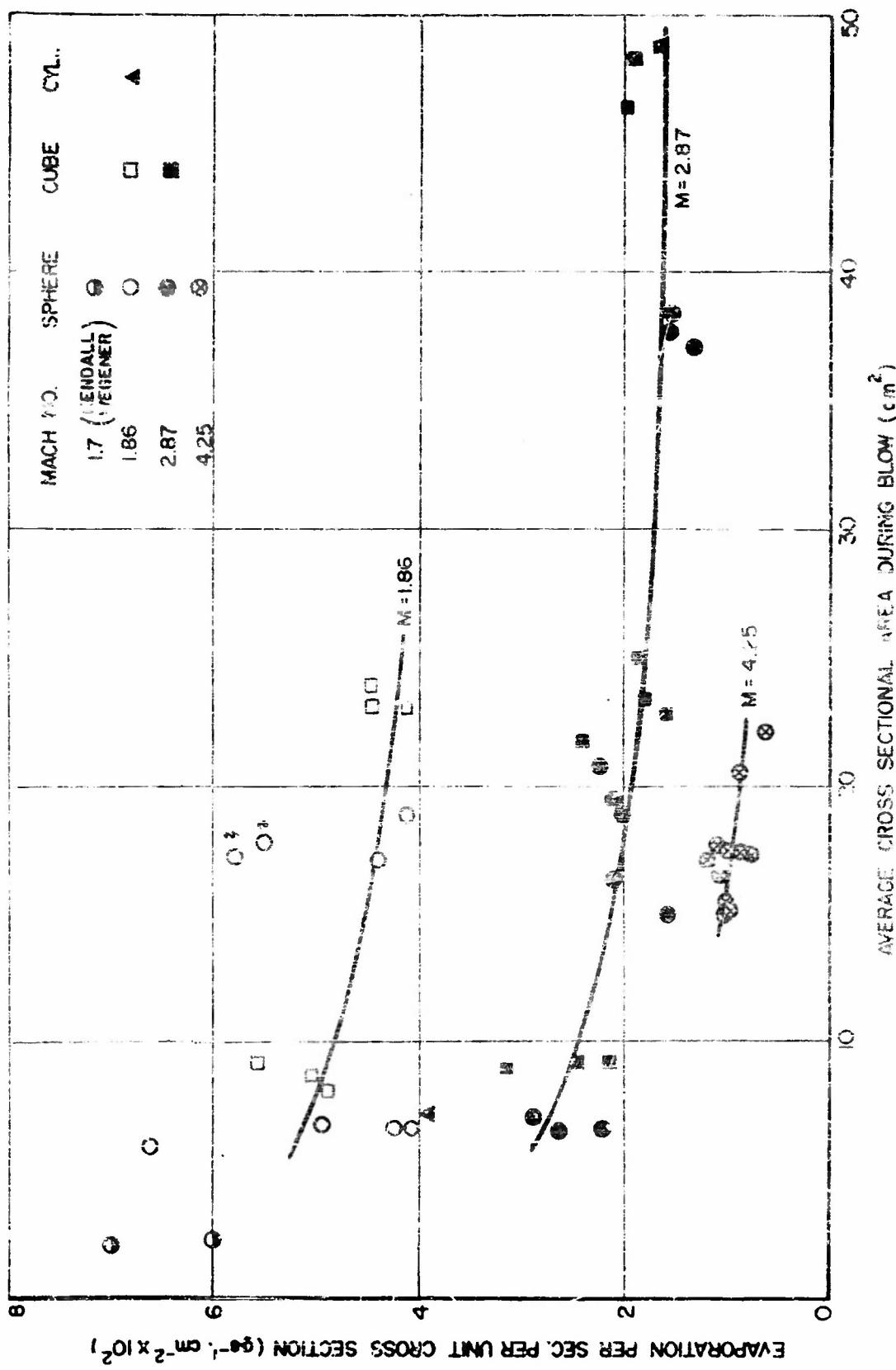
FIG. 4 EVAPORATION OF CUBES AND SPHERES OF DRY ICE AT DIFFERENT MACH NUMBERS VS CROSS SECTIONAL AREA OF THESE BODIES

Aeroballistic Research Department
External Distribution List for Aeroballistics Research (XI)

No. of
Copies

Chief, Bureau of Ordnance
Department of the Navy
Washington 25, D.C.
1   Attn: Rea
1   Attn: Rexc
1   Attn: Re3d
2   Attn: Re6
3   Attn: Re9a

Chief, Bureau of Aeronautics
Department of the Navy
Washington 25, D. C.
1   Attn: AER-TD-414
2   Attn: RS-7

Commander
U. S. Naval Ordnance Test Station
Inyokern
P.O. China Lake, California
2   Attn: Technical Library
1   Attn: Code 5003

Commander
U.S. Naval Air Missile Test Center
Point Mugu, California
2   Attn: Technical Library

Superintendent
U.S. Naval Postgraduate School
Monterey, California
1   Attn: Librarian

Commanding Officer and Director
David Taylor Model Basin
Washington 7, D. C.
2   Attn: Hydrodynamics Laboratory

Chief of Naval Research
Library of Congress
Washington 25, D. C.
2   Attn: Technical Info. Div.

Office of Naval Research
Department of the Navy
Washington 25, D. C.
1   Attn: Code 438
2   Attn: Code 463

Director
Naval Research Laboratory
Washington 25, D. C.
1   Attn: Code 2021
1   Attn: Code 3800

1   Officer-in-Charge
Naval Aircraft Torpedo Unit
U.S Naval Air Station
Quonset Point, Rhode Island

Office, Chief of Ordnance
Washington 25, D. C.
1   Attn: ORDTU

No. of
Copies

2   Library Branch
Research and Development Board
Pentagon 3D1041
Washington 25, D.C.

Chief, AFSWP
P.O. Box 2610
Washington 25, D. C.
1   Attn: Technical Library

1   Chief, Physical Vulnerability Branch
Air Targets Division
Directorate of Intelligence
Headquarters, USAF
Washington 25, D. C.

Commanding General
Wright Air Development Center
Wright-Patterson Air Force Base
Dayton, Ohio
5   Attn: WCAPD
1   Attn: WCSD
2   Attn: WCSOR
2   Attn: WCRRN
1   Attn: WCACD
1   Attn: WCRRF

1   Director
Air University Library
Maxwell Air Force Base, Alabama

Commanding General
Aberdeen Proving Ground
Aberdeen, Maryland
1   Attn: C.L. Poor
1   Attn: D.S. Dederick

National Bureau of Standards
Washington 25, D.C.
1   Attn: Nat'l Applied Math. Lab.
1   Attn: Librarian (Ord. Dev. Div.)
1   Attn: Chief, Mechanics Div.

National Bureau of Standards
Corona Laboratories (Ord. Dev. Div.)
Corona, California
1   Attn: Dr. H. Thomas

National Bureau of Standards
Building 3U, UCLA Campus
405 Hilgard Avenue
Los Angeles 24, California
1   Attn: Librarian

University of California
711 Mechanics Building
Berkeley 4, California
1   Attn: Dr. R. G. Folsom
1   Attn: Mr. G. J. Maslach
1   Attn: Dr. S. A. Schaaf
VIA: InsMat

North American Aviation, Inc.
12214 Lakewood Boulevard
Downey, California
2   Attn: Aerophysics Library
      VIA: BuAero Representative

United Aircraft Corporation
East Hartford 8, Connecticut
1   Attn: Robert C. Sale
      VIA: BuAero Representative

National Advisory Committee for Aero
1724 F Street, Northwest
Washington 25, D. C.
5   Attn: E. B. Jackson

Ames Aeronautical Laboratory
Moffett Field, California
1   Attn: H. J. Allen
2   Attn: Dr. A.C. Charters

NACA Lewis Flight Propulsion Lab.
Cleveland Hopkins Airport
Cleveland 11, Ohio
1   Attn: John C. Evvard

Langley Aeronautical Laboratory
Langley Field, Virginia
1   Attn: Theoretical Aerodynamics Div.
1   Attn: J. V. Becker
1   Attn: Dr. Adolf Buseman
1   Attn: Mr. C. H. McLellan
1   Attn: Mr. J. Stack

Harvard University
21 Vanserg Building
Cambridge 38, Massachusetts
1   Attn: Prof. Garrett Birkhoff

The Johns Hopkins University
Charles and 34th Streets
Baltimore 18, Maryland
1   Attn: Dr. Francis H. Clauser

New York University
45 Fourth Avenue
New York 3, New York
1   Attn: Professor R. Courant

1   Dr. Allen E. Puckett, Head
Missile Aerodynamics Department
Hughes Aircraft Company
Culver City, California

1   Dr. Gordon N. Patterson, Director
Institute of Aerophysics
University of Toronto
Toronto 5, Ontario, Canada
      VIA: BuOrd (Ad8)

No. of
Copies

5 Office of Naval Research
Branch Office
Navy 100
Fleet Post Office
New York, New York

  Commanding General
Aberdeen Proving Ground
Aberdeen, Maryland
1 Attn: Dr. B L. Hicks

  National Bureau of Standards
Aerodynamics Section
Washington 25, D C
1 Attn: Dr. G.B Schubauer, Chief

  Ames Aeronautical Laboratory
Moffett Field, California
1 Attn: Walter G. Vincenti

  University of California
Observatory 21
Berkeley 4, California
1 Attn: Leland E. Cunningham
  VIA: InsMat

  Massachusetts Inst. of Technology
Dept. of Mathematics. Room 2-270
77 Massachusetts Avenue
Cambridge, Massachusetts
1 Attn: Prof. Eric Reisaner
  VIA: InsMat

  Graduate School Aeronautical Engr.
Cornell University
Ithaca, New York
1 Attn: W.R. Sears, Director
  VIA: ONR

  Applied Math. and Statistics Lab.
Stanford University
Stanford, California
1 Attn: R.J. Langie, Associate Dir.
  VIA: Ass't InsMat

  University of Minnesota
Dept. of Aeronautical Engr.
Minneapolis, Minnesota
1 Attn: Professor R. Hermann
  VIA: Ass't InsMat

  Case Institute of Technology
Dept. of Mechanical Engineering
Cleveland, Ohio
1 Attn: Professor G. Kuerti
  VIA: ONR

  Harvard University
109 Pierce Hall
Cambridge 33, Massachusetts
1 Attn: Professor R. von Mises

No. of
Copies

   1   Prof. E. R. G. Eckert
          Department of Mechanical Engineering
          University of Minnesota
          Minneapolis 14, Minnesota

   1   Prof. F. L. Whipple
          Harvard College Observatory
          60 Garden Street
          Cambridge 38, Massachusetts

   1   Dr. Richard N. Thomas
          Harvard College Observatory
          60 Garden Street
          Cambridge 38, Massachusetts

   1   Dr. G. R. Eber
          Holloman Air Development Center
          Alamogordo, New Mexico

   1   Dr. P. P. Wegener
          Jet Propulsion Laboratory
          4800 Oak Grove Drive
          Pasadena, California